2 Towards a dark matter experiment

C. Amsler, V. Boccone, H. Cabrera, S. Horikawa, P. Lightfoot[3], C. Regenfus, and J. Rochet

in collaboration with:
CIEMAT, ETHZ, Soltan Institute (Warsaw), Universities of Granada and Sheffield

(ArDM Collaboration)

In 2006 we continued the development of the light readout system for the ArDM dark matter experiment. We plan to use a one ton liquid argon time projection chamber to detect recoil nuclei from the scattering of Weak Interacting Massive Particles. WIMPs are among the favorite candidates for the missing non-baryonic matter in the universe, and the prominent candidate is the lightest supersymmetric (SUSY) particle, the neutralino, with a mass of at least 40 GeV. The experimental upper limit for the cross-section of WIMPs with nucleons is about 10^{-6} pb, a cross section that would lead to 100 events per day in the ArDM detector, assuming a detection threshold of 30 keV for recoil argon nuclei.

Details on the experiment can be found in our previous annual report and in ref. (1). The drifting electron charge from ionizing recoils and the VUV scintillation light (128 nm) will be recorded with high efficiency to suppress the electron background from the radioactive β-emitter ^{39}Ar. Its activity in natural ^{40}Ar argon has been measured to be about 1 Bq/kg (2), therefore inducing a background rate of about 1 kHz in a one ton detector. The rejection of the γ- and β-background will be achieved through the combined measurement of the charge-to-light ratio, the time structure of the light signal, and the determination of the interaction point on an event-by-event basis.

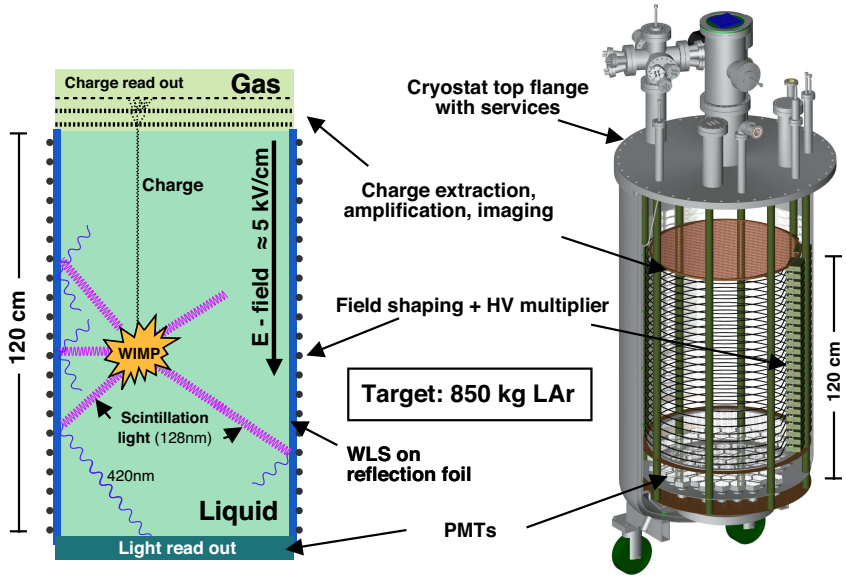

Figure 2.1: Detection principle and 3D-drawing of the ArDM detector.

[3]Visitor from the University of Sheffield

The ratio of primary scintillation light to ionization charge collected after a given drift time in an external electric field is different for nuclear recoils and minimum ionizing particles, being very high for the former, due to quenching. This provides the main discrimination between WIMPs and background. On the other hand, the VUV photons are produced from the spin singlet and triplet states of the excited dimer A_2^*, following ionization, which have different lifetimes (τ = 7 ns, resp. 1.6 μs in liquid (3)). These states are populated differently according to the excitation process: for heavy ionization (such as nuclear recoils) the singlet dominates, while for minimum ionizing particles (such as electrons) the triplet dominates (3). Hence the discrimination of decay time allows a further separation between WIMP induced recoils and background from γ or electrons.

The working principle of the two-phase detector is shown in Fig. 2.1 (left). A WIMP interaction leading to 30 keV recoils produces about 400 VUV photons, together with a few free electrons. The strong vertical electric field (5 kV/cm) sweeps the electrons to the top surface of the liquid and extracts them into the gas phase. After multiplication ($\approx 10^5$) in a two stage Large Electron Multiplier (LEM) the charges are collected by a segmented anode. The VUV light is emitted isotropically from the interaction point and converted to blue light by a wavelength shifter (WLS) on the side walls. The shifted and reflected light is collected at the bottom of the cryostat by 14 phototubes (8") immersed in the liquid. The 3D-CAD sketch (Fig. 2.1, right) shows the mechanical design of the prototype detector and the cryostat. Not shown is the (non-conductive) wavelength shifting foil inside the field shapers.

2.1 Photomutiplier operation at low temperature

Low temperature photomultipliers (PMTs) covering a surface of ≈1.5 m^2 and immersed in liquid argon will be used in the ArDM experiment. A bialkali photocathode has a quantum efficiency of typically 30% at room temperature, but becomes insulant at liquid argon temperatures (≈ 88K). A platinum (Pt) underlay under the photocathode is necessary to restore the electron population in the photocathode. Unfortunately, this solution also reduces the quantum efficiency to ≈15%.

We have investigated two 3" PMTs for their functionality and quantum efficiency at low temperature. The best result was obtained with a square 8-dynode tube from Hamamatsu (R6237-MOD) manufactured with Pt-underlay. The dark current (thermal emission rate × gain) and the response to light (gain) were measured. Figure 2.2 shows the expected decrease of dark current for the Hamamatsu tube at low temperature, while the light response remains constant (the slight increase in Fig. 2.3 is attributed to a gain fluctuation).

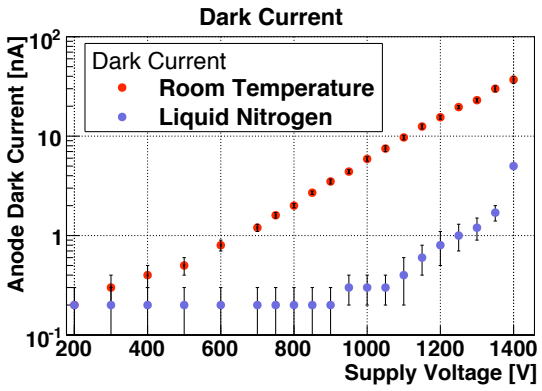

Figure 2.2: Dark current vs. bias voltage for room and liquid N_2 temperature.

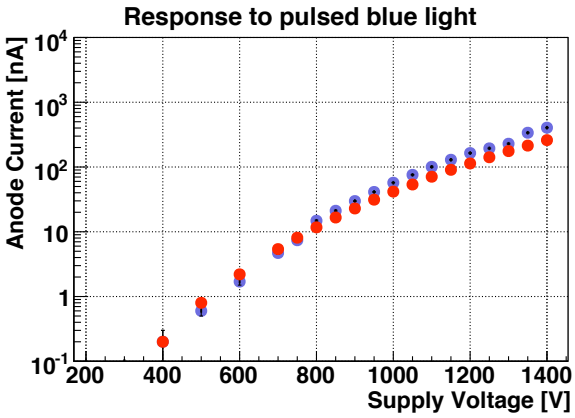

Figure 2.3: Response to blue light of the Hamamatsu PMT vs. bias for room (red dots) and liquid N_2 (blue dots) temperature.

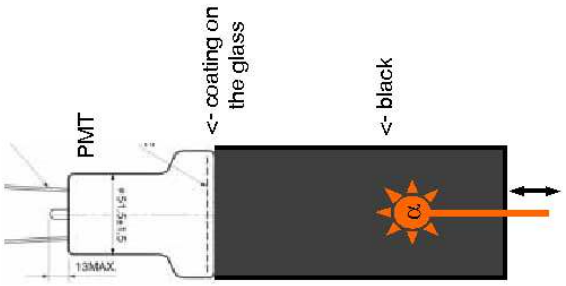

Figure 2.4: Experimental setup.

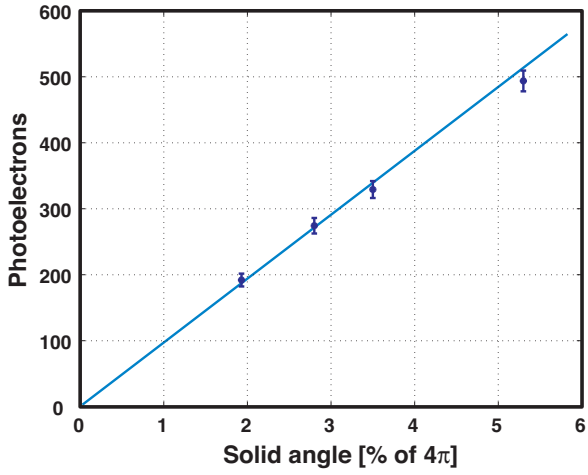

Figure 2.5: Number of photoelectrons from the 5.3 MeV α-source as a function of the solid angle subtended by the Hamamatsu R6237-MOD PMT in argon gas.

To optimize the light collection efficiency we performed various measurements with different setups, reflectors material and WLS. For example, the glass window of PMTs can be coated with a WLS within a matrix of paraloid or polystyrene (4), giving thin transparent wavelength shifting layers. Light emitted from the WLS in the (optically dense) matrix is trapped and efficiently produces photoelectrons at the photocathode. Efficient conversion of VUV light was observed by coating the PMT glass surface with tetraphenyl-butadiene (TPB) dissolved in paraloid or polystyrene (PS). The layer (1 μm thickness) was deposited by dissolving TPB/PS in chloroform and dipping the PMT in the solution. A black box filled with argon gas and a 5.3 MeV movable α-source were used (Fig. 2.4). The number of photoelectrons was measured for different distances between the PMT and the α-source. As expected, the data expressed as a function of solid angle is compatible with a straight line. We obtained 480 photoelectrons for a 5% solid angle, which corresponds to a quantum efficiency of about 12%.

2.2 Light yield in argon

We have determined the light yield in gaseous and liquid argon and established the ratio of singlet to triplet contributions. Our measurements in gas with a 5ℓ vacuum chamber showed that the number of photoelectrons depends crucially on the purity of argon, the contribution from the slow component and its decay time increasing with purity (see our previous annual report). The two decay components were clearly observed with a mean life of 15.7 $\pm$ 4.0 ns for the fast (singlet) and 3.12 $\pm$ 0.08 μs for the slow (triplet) component (5). The latter is in good agreement with literature, 3.2 $\pm$ 0.3 μs (6). A first attempt to measure the singlet to triplet population ratio in liquid is shown in Fig. 2.6. The plots show the ratio R of fast ($<$ 50 ns) to total light output vs. total amplitude for the Po α-source (left) and with

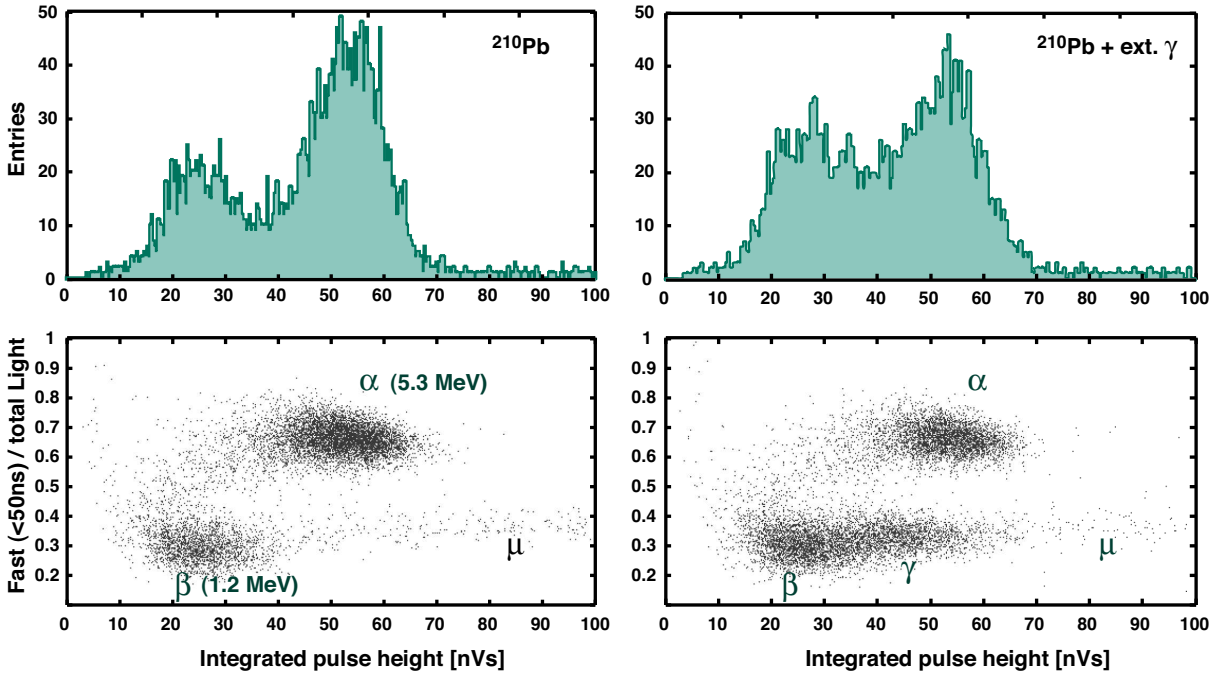

Figure 2.6: Ratio R of fast to total light output vs. time integrated amplitude with (left) and without (right) external γ source.

an additional external γ-source (right). One observes a clear separation between heavily ionizing projectiles and electrons.

Figures 2.7 and 2.8 show the improved apparatus built in 2006. Two Hamamatsu (R6237-MOD) PMTs face one another. The cell volume is roughly 1ℓ and an α-source is located in the center. The PMT glass surfaces are coated with a transparent TPB/paraloid layer. The side walls consist of 10×10 cm^2 foils with evaporated TPB. The analogue signal from the PMT is sampled by a 1 GHz digital oscilloscope, stored to hard disk and analysed offline.

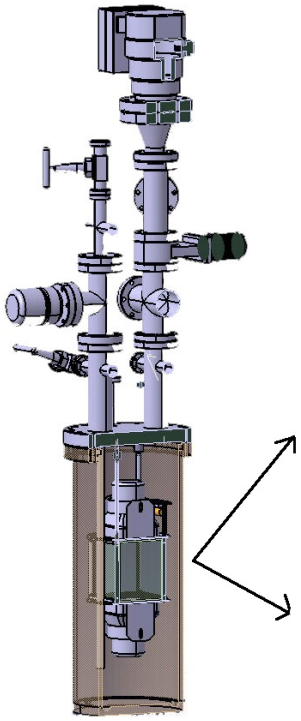

Figure 2.7: 2006 setup.

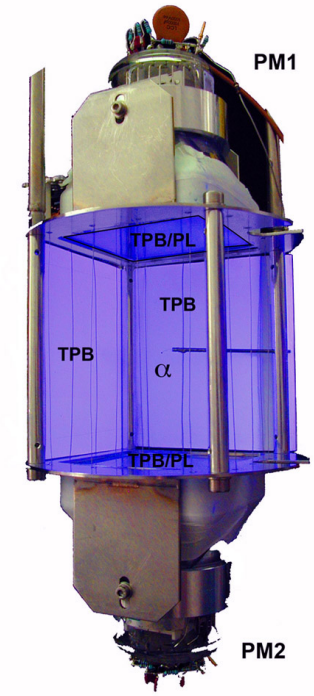

Figure 2.8: Enhanced view of the liquid argon cell cell under UV illumination.

A baseline correction is performed with the portion of the signal before trigger time. The noise is determined by the amplifier. The number of detected photons is calculated as usual by dividing the integrated charge by the average single photon charge, which we find from distributions of dark counts and LED light pulses.

From several measurements with the old and the new setup we find an average value for the triplet to singlet ratio of 6.0 $\pm$ 1.8 for 5.3 MeV α in argon gas at NTP. The error was estimated from fluctuations among the data sets. The largest measured value for the triplet decay time τ_2 = 3.12 μs, mentioned above, was found for the purest argon gas. Impurities in argon gas were found to reduce the scintillation light by shortening the decay time τ_2. This effect was studied in detail by mixing argon gas with air at partial pressures between 1 and 10^{-6} mbar (5). For the various partial air pressures the averaged α-signals were fitted and analysed, as described above. Figure 2.9 shows the yields obtained for the fast and slow components vs. τ_2. The contribution from the slow component increases linearly with τ_2, reaching to 3.2 μs in gas at NTP, while the fast component remains constant. This behaviour can be explained as due to the non-radiative destruction of the triplet excimer states by gas impurities. This is presumably due to residual water, since cooling improves on the light yield (and τ_2).

Figure 2.10 shows measurements done with different coatings and reflectors. From the known yield of VUV photons (78 k / α-particle (7)), we find the detection efficiencies (defined as the ratio of detected photoelectrons to emitted UV photons) for the different designs by extrapolating to τ_2 = 3.2 μs. The best result (1% detection efficiency) was achieved with TPB evaporated on 3M reflective foils.

Evaporation leads to a much more uniform coating than spraying (Fig. 2.11). We have de-

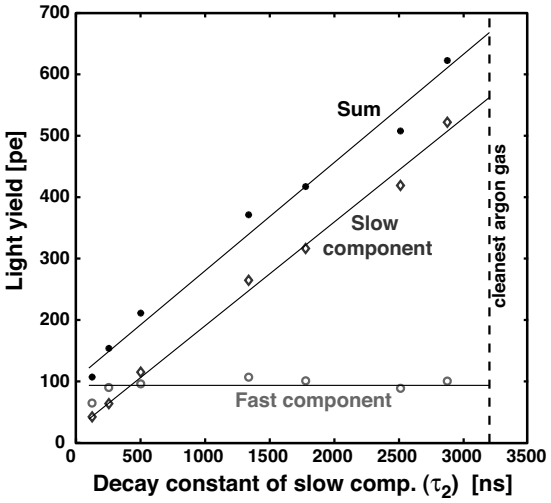

Figure 2.9:
Light yield (number of photoelectrons) in gaseous argon (NTP) as a function of τ_2. The measurements correspond to different partial air pressures.

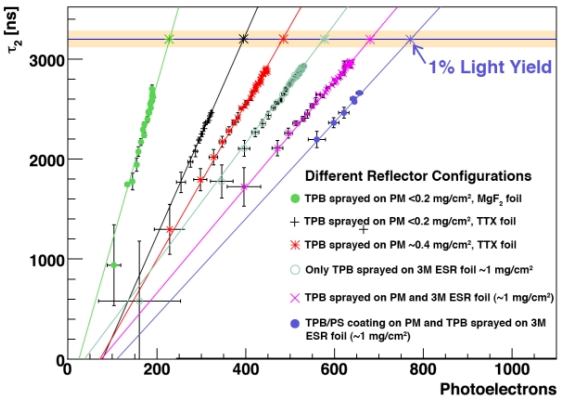

Figure 2.10: τ_2 vs. number of photoelectrons for various coatings and reflectors.

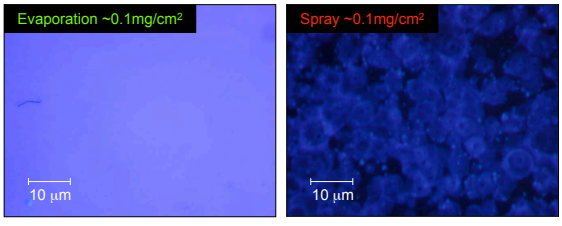

Figure 2.11: Microscope comparison between evaporated and sprayed TPB, illuminated by UV light.

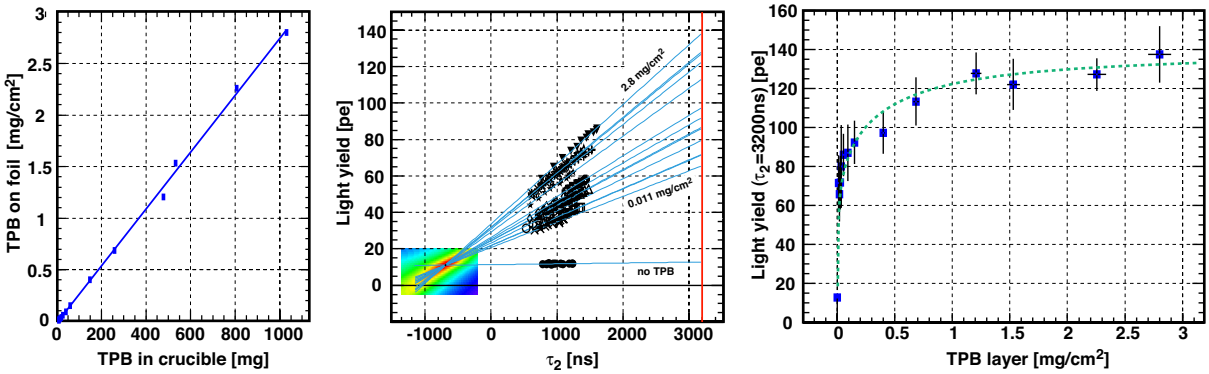

Figure 2.12: Left: TPB thickness vs. mass in crucible. Middle: number of photoelectrons vs. τ_2. Right: number of photoelectrons vs. TPB thickness. The dashed line is drawn to guide the eye.

termined the optimum thickness of TPB wavelength shifter to be evaporated on the 3M reflector by using the black box setup shown in Fig. 2.4. A small glass exsicator was modified to include a heated crucible. The layer thickness of TPB was calculated by weighing the foil before and after vacuum evaporation. Figure 2.12 (left) shows the expected linear correlation between the deposited thickness and the mass of TPB prepared in the crucible, which demonstrates the reliability of the procedure. Figure 2.12 (middle) shows the light yield as a function of τ_2 (hence gas purity) for various TPB thicknesses. The straight lines are fits to a common intersection point. Extrapolation to τ_2 = 3.2 μs lead to the expected light yield for 100% argon purity. The latter is shown as a function of TPB thickness in Fig. 2.12 (right). Saturation is observed above 1 mg/cm^2 which corresponds to a film of about 10 μm thickness.

A similar correlation between light yield and τ_2 seems to be observed in liquid argon and is the subject of our present investigations. The goal is to collect enough light in liquid to distinguish between nuclear recoils and electrons and to measure the suppression factor for ^{39}Ar background events. In liquid the light output from the α-emitter is quenched by the strong dE/dx and one expects about 15 photons / keV (or 450 photons from a recoiling nucleus of 30 keV), while a minimum ionizing particle leads to 40 photons / keV in the absence of electric field (8).

Our R&D developments for the VUV light yield are encouraging for a large detector volume, the goal being to reach 2%, while 1% has already been achieved. We will therefore proceed with the construction of the one ton prototype in 2007.

[1] C. Regenfus, Proc. 6th Int. Workshop on the Identification of Dark Matter (IDM06), Rhode Island, World Scientific, 2006.

[2] P. Benetti et al. (WARP Collaboration), preprint astro-ph/0603131 (2006).

[3] A. Hitachi et al., Phys. Rev. **B 27** (1983) 5279.

[4] G. Eigen, E. Lorenz, Nucl. Instr. Meth. **166** (1979) 165.

[5] A. Büchler, Bachelor Thesis, Universität Zürich (2006).

[6] J. Keto et al., Phys. Rev. Lett. **33** (1974) 1365.

[7] R. Chandrasekharan et al., Nucl. Instr. Meth. in Phys. Res. **A 546** (2005) 426.

[8] P. Cennini et al., Nucl. Instr. Meth. in Phys. Res. **A 432** (1999) 240.